Fluorescence relaxation in intact cells of photosynthetic bacteria: donor and acceptor side limitations of reopening of the reaction center

Emese Asztalos · Gábor Sipka · Péter Maróti

The publisher's version is available: Photosynth Res 2015 Apr;124(1):31-44; DOI 10.1007/s11120-014-0070-0

Abstract

The dark relaxation of the yield of variable BChl fluorescence in the 10^{-5}–10 s time range is measured after laser diode (808 nm) excitation of variable duration in intact cells of photosynthetic bacteria Rba. sphaeroides, *Rsp. rubrum*, and *Rvx. gelatinosus* under various treatments of redox agents, inhibitors, and temperature. The kinetics of the relaxation is complex and much wider extended than a monoexponential function. The longer is the excitation, the slower is the relaxation which is determined by the redox states, sizes, and accessibility of the pools of cytochrome c_2^{2+} and quinone for donor and acceptor side-limited bacterial strains, respectively. The kinetics of fluorescence decay reflects the opening kinetics of the closed RC. The relaxation is controlled preferentially by the rate of re-reduction of the oxidized dimer by mobile cytochrome c_2^{2+} in *Rba. sphaeroides*and *Rsp. rubrum* and by the rate constant of the Q_A interquinone electron transfer, $(350\mu s)^{-1}$ and/or the quinol/ quinone exchange at the acceptor side in *Rvx. gelatinosus*. The commonly used acceptor side inhibitors (e.g., terbutryn) demonstrate kinetically limited block of re-oxidation of the primary quinone. The observations are interpreted in frame of a minimum kinetic and energetic model of electron transfer reactions in bacterial RC of intact cells.

Introduction

The cytoplasmic membrane system of purple bacteria includes the photosynthetic apparatus that converts the light energy to electrochemical potential (Wraight 2004; Niederman 2006; Tucker et al. 2010). The light-harvesting (antenna) complexes (LH) absorb photons, and funnel the electronic excitation to the reaction center (RC) protein where charge separation and subsequently a series of electron transfer reactions take place (Fig. 1). The RC houses a homologous pattern of cofactors and protein arrangements with strong twofold symmetry. The heterodimer of similar L and M subunits binds all the active cofactors: four bacteriochlorophylls (BChls), two bacteriopheophytins (Bphe), two quinones (Q) and a non-heme iron atom (Fe). Although the two branches of cofactors show a high degree of rotational symmetry, the electron transfer from the primary donor P to the secondary quinone Q_B via $BChl_A$, $BPhe_A$, and Q_A occurs exclusively through the A branch. The structural and compositional symmetry contrasts with additional functional asymmetry. While the two quinones are chemically identical, their properties are very different: Q_A is a tightly bound and one-electron redox agent and Q_B is a reversibly bound and two-electron redox species. The H subunit which stabilizes the whole complex is enriched with water molecules at the cytoplasmic side and facilitates proton uptake coupled to the electron transfer. The fast initial electron transfer steps on the donor and acceptor sides decrease the chance of wasteful recombination of the light-induced separated charges. The products of the charge stabilization in the RC are the double reduced QH_2 and the single oxidized cyt c^{3+} that are exported into the membrane and the aqueous periplasmic side of the RC, respectively. They act as electron transfer shuttles between two membrane bound proteins, the RC and the cytochrome bc_1 complexes.

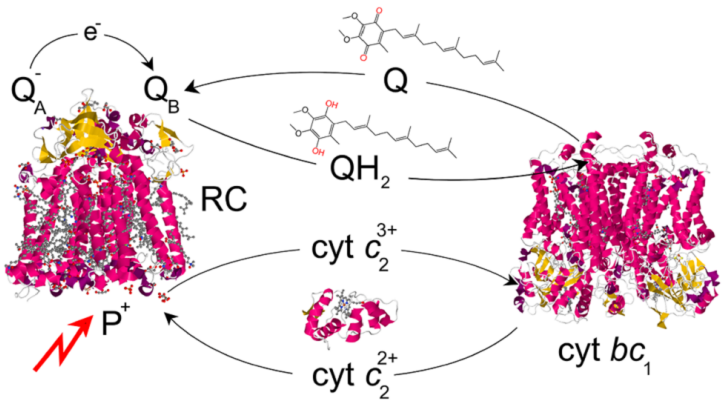

Fig. 1 Schematic demonstration of light-induced cyclic electron flow between RC and cyt bc_1 complexes via mobile electron carriers cyt c_2 in the aqueous phase and Q in the membrane in photosynthetic apparatus of purple bacterium Rba. sphaeroides.

The stoichiometry of the participants is arbitrary. The coordinates of the proteins are from 3I4D.pdb (RC), 2FYN.pdb (cyt bc_1), and 1CXC.pdb (cyt c_2)

The organization of the complexes resulting in the physiological function of the apparatus has been characterized by high atomic resolution and at an unprecedented level of biochemistry and physical chemistry (Bahatyrova et al. 2004; Sener et al. 2007; Sener and Schulten 2009; Cartron et al. 2014). Although the functional studies including the efficient light-induced cyclic electron transfer among the complexes require compact organization of the components (Comayras et al. 2005; Lavergne et al. 2009), the high-resolution structural [atomic force microscopy (AFM)] analysis offers controversial results about cytochrome bc_1 complexes in the membrane areas of the core complexes (Scheuring 2009; Sturgis and Niederman 2009; Cartron et al. 2014). The problem of arrangement and degree of connectivity of the photosynthetic molecular complexes has not been yet settled. Vermeglio et al. (1993) observed that the RC-LH1 complexes in intact cells of *Rba. sphaeroides*strain Ga were organized in dimeric structure dictated by the neurosporene-type carotenoids (D'Haene et al. 2014). Joliot et al. (1989) proposed supramolecular arrangement of 2 RCs (dimer), 1 cyt c_2 and 1 cyt bc_1 in intracytoplasmic membrane (ICM) of *Rba. sphaeroides*R26 supported by numerous biochemical and AFM studies (Francia et al. 1999). The concept of supercomplex organization has been accepted with strong critics (Crofts et al. 1998). In the cytoplamic membrane (CM) no supercomplexes have been assumed as the cytochromes c_2 (~7 cyt c_2/RC) and cyt bc_1 complexes are shared with the respiratory chains (Vermeglio and Joliot 2014). During adaptation to low-light intensity in *Rba. sphaeroides*cells, the absorption cross section increases, but the RC electron transfer turnover is slowing down, due to the slower diffusion of ubiquinone between the RC and the cyt bc_1 complex, which is caused by the dense packing of LH2 rings in the lipid bilayer (Woronowitz et al. 2011). Similar effect was observed during transition from aerobic to anaerobic conditions (greening) of the *Rba. sphaeroides*cells (Koblizek et al. 2005; Kis et al. 2014). These findings do not support the supercomplex model. According to Cartron et al. (2014), restricted electron transfer domains are likely to exist, but not as fixed RC-LH1-PufX-cyt bc_1 supercomplexes. Instead, cyt bc_1 complexes sit adjacent to RC-core complexes in disordered areas but with no direct contact with the majority of the RC-LH1-PufX complexes. The organization of the complexes in the membrane and the rates of export of charges from the RC determine the reopening time of the closed RC that is an essential parameter of energy utilization of the photosynthetic apparatus exposed to continuous illumination. Faster re-opening of the RC enables higher turnover rate of the system. The RC remains closed for excitation as long as the charges on the oxidized BChl dimer (P+) and on the reduced primary quinone (Q_A) do not disappear. In PSII of green plant photosynthesis, the rate of re-reduction of P+ is much greater than that of the interquinone ($Q_A^- Q_B \rightarrow Q_A Q_B^-$) electron transfer; therefore, the kinetics of re-opening of the PSII RC follows that of the export of the electrons via the quinone acceptor complex (Bukhov et al. 2001; Cser and Vass 2007). In bacterial systems, the situation is much more complicated. The electron donors to P+ (reduced cytochromes) can either be attached to the RC and form separate subunit (e.g., Bla. viridis and *Rvx. gelatinosus*) or are docked at distal or proximal locations of the RC (e.g., Rba. sphaeroides) and/or are available after (prolonged) diffusion only (e.g., *Rsp. rubrum*). Additionally, the variable RC/cyt c_2 stoichiometry extends the kinetics of P+ re-reduction (P^+cyt $c_2^{2+} \rightarrow$ P cyt c_3^{2+}) from micro- to millisecond time range that can coincide with that of the interquinone electron transfer. We have fairly firm knowledge about the interquinone electron transfer in isolated RCs from *Rba. sphaeroides*(for reviews see Okamura et al. 2000; Wraight and Gunner 2009): the conformation limited first transfer ($Q_A^- Q_B \rightarrow Q_A Q_B^-$) is more than one order of magnitude faster than the proton-activated second electron transfer, $Q_A^- Q_B^- \rightarrow Q_A Q_B H_2$ (~10^3 s^{-1} at pH 8). We are uncertain whether this is true in intact cells and other strains because in chromatophore membrane of Rba. capsulatus, Lavergne et al. (1999) found that the first and second interquinone electron transfers exhibited essentially identical kinetic properties both with rates in the 100 μs^{-1} range including the associated protonation reactions. It is a great challenge to find the conditions (time range, duration and intensity of the excitation, redox state of the RC, strain of the bacterium, etc.) for the rate-limiting steps of the opening of the closed RC in intact bacterial cells. The fluorescence emission from the antenna BChl pigments is controlled by the activity of the RC depending on its redox state and on the organization of the photosynthetic unit. As the closed and open states of the RC are characterized by high and low levels of BChl fluorescence, respectively (Vredenberg and Duysens 1963; van Grondelle 1985), their interchange can be followed by tracking the yield of the variable fluorescence. Clayton (1966) showed in a variety of cells that the relationship between fluorescence yield and oxidation of the RC dimer observed by Vredenberg and Duysens (1963) in *Rsp. rubrum* cells was limited to aerobic conditions, and that under anaerobiosis the fluorescence yield was controlled by events on the electron acceptor side. Rivoyre et al. (2010) measured the relaxation of fluorescence of a blocked RC in the time range of seconds after flash excitation and studied the energetic coupling among the photosynthetic units. Kocsis et al. (2010) demonstrated

but did not analyze the diversity of fluorescence decay kinetics of several bacterial strains measured by a kinetic BChl fluorometer based on excitation by pulsed laser-diodes of variable duration. The photosynthetic membrane showed characteristic fluorescence changes during different stages of development (aging) (Asztalos et al. 2010a), bleaching and greening of the ICM (Kis et al. 2014), and mercury treatment (Asztalos et al. 2010b, 2012) of Rba. sphaeroides. Kolber et al. (1998) introduced the fast repetition fluorometer where the single and multiple turnover excitation evoked by LED was controlled by the number of submicrosecond non-saturating flashes (''flashlets'') followed by relaxation. The decay of the fluorescence was attributed exclusively to re-oxidation of Q_A^- in the quinone acceptor complex (Kolber et al. 1998) that can be true for study of marine ecosystem (Falkowski et al. 2004; Hohmann-Mariott and Blankenship 2007) but highly questionable to draw conclusions about membrane development in *Rba. sphaeroides*(Koblizek et al. 2005). The few previous works clearly indicate the importance of this field which is far away from understanding. Here, we will demonstrate that the kinetics of fluorescence relaxation can show different faces depending on the intensity and duration of the excitation and on the competition between Q_A^- oxidation and P+ re-reduction reactions. The systematic study will reveal the nature of the relaxation of BChl fluorescence in intact cells of different bacterial strains. The fluorescence measurements will be combined with redox titration and with measurements of light-induced absorption changes under different experimental conditions. It will be shown how the BChl dark relaxation can be used as readily available and sensitive tool to characterize the RC controlled electron transfer in different bacterial strains under various light and redox conditions.

Materials and methods

Chemicals, bacterial strains and growth

Cells of purple non-sulfur photosynthetic bacterium Rhodobacter (Rba.) sphaeroides strain 2.4.1 (Maróti and Wraight 1988), Rhodospirillum (Rsp.) rubrum, Rubrivivax (Rvx.) gelatinosus (Vermeglio et al. 2012), and Blastochloris (Bla.) viridis (Blankenship et al. 1995; Konorty et al. 2009) were cultivated anaerobically in Siström medium (Siström 1962) in 1 l screw top flasks under continuous illumination of about 13 W m^{-2} provided by tungsten lamps (40 W). *Rvx. gelatinosus* cells were obtained from Prof. Dr. A. Vermeglio, CEA Laboratoire de Bioenerge´tique Cellulaire, Saint-Paul-lez-Durance, France. The cytochrome c_2 deficient mutant of *Rba. sphaeroides*(CYCAI, generous gift from Dr. Donohue, University of Wisconsin, Madison, Wisconsin USA) was cultivated in the dark on a shaker (1 Hz) in the presence of antibiotic kanamycin and spectinomycin. The bacteria were harvested in the late stationary phase of the cell growth and bubbled by nitrogen for 15 min before measurements. The optical density of the samples was kept low [OD (808 nm)\ 0.1] to keep the secondary effects (scattering, re-absorption of BChl fluorescence, secondary fluorescence, etc.) negligible compared to the primary signals. The BChl used for reference in fluorescence relaxation measurements was extracted from the cells by acetone/ methanol (7:2 v/v) mixture. Reduced TMPD (N,N,N_0,N_0-tetramethyl-p-phenylenediamine, E_m ~270 mV) or ferrocene (E_m ~420 mV) was used as external electron donors for the RC if the endogenous donor (cyt c_2) is absent (CYCAI) or is present in small amount. They are efficient donors and prevent accumulation of the states $P^+Q_A^-$ or $P^+Q_A^{-2}$ upon intensive and long illumination. The ubiquinone pool and the acceptor side of the RC were reduced gradually by adding increasing amount of sodium dithionite up to 20 mM in darkadapted cells flushed with nitrogen. During all experiments the temperature was controlled at 293 K if otherwise not indicated.

Redox titration

Titrations of P and the cytochrome c_2 pool were performed in our kinetic absorption spectrophotometer using the homebuilt redox cell as described (Maróti and Wraight 1988). The measuring platinum electrode and the Ag/AgCl reference electrode in 3M KCl were fitted to the 1 cm 9 1 cm cuvette equipped by a stirring bar. The typical medium contained the following redox mediators: 4 μM phenazine ethosulphate, 4 μM phenazine methosulphate, 40 μM TMPD, 40 μM 2,6- dichlorophenolindophenol, 20 μM 1,2-naphtoquinone, 20 μM 1,4-naphtoquinone, 20 μM 2,5-dihydroxy-p-benzoquinone, and 20 μM anthraquinone sulphonate. The relative amount of oxidized P and cyt c_2 at each potential was determined from the magnitude of a flash-induced absorption change at 798 and 551 nm (with reference to 570 nm), respectively. Reductive titrations were performed by the addition of aliquots of 1 mM dithionate freshly prepared, and oxidative titrations with 150 mM ferricyanide. Before each measurement, a minimum of 5 min equilibration was allowed to accommodate the sample to the actual redox potential.

Light-induced absorption change

The cells were re-suspended in fresh medium and anaerobically adapted in the dark for 15 min prior measurement. The kinetics of absorption changes of the whole cells induced by Xe flash (3-ls half-time duration) or by laser diode (Roithner LaserTechnik LD808-2-TO3, wavelength 808 nm and power 2 W) of rectangular shape with variable duration was detected by a home-constructed spectrophotometer (Maróti and Wraight 1988). The kinetics of oxidized dimer (P+) was tracked at 798 nm (Bina et al. 2009; Rivoyre et al. 2010). The light-induced energetization of the membrane was monitored by electrochromic band shift of carotenoids at 540 nm (Asztalos et al. 2012; Kis et al. 2014). A flow cuvette was applied for repetitive measurements with bacteria of impeded electron transfer resulting in long-lived trapped RC state (e.g., CYCAI with acceptor side inhibitor). The opening of the closed RC was tested by double flash experiments: the saturating first (Xe) flash closed the RC and the initial absorption change caused by a second saturating flash with variable delay relative to the first one monitored the kinetics of re-opening of the RC.

Fluorescence

The induction of BChl prompt fluorescence yield (Maróti 2008; Maróti and Wraight 2008) and the decay of the yield of the fluorescence (Kocsis et al. 2010) were measured by home-made kinetic BChl fluorometers. The bacteria were excited by pulsed laser diode (Roithner LaserTechnik LD808-2-TO3, wavelength 808 nm and power 2 W) of variable duration, and the BChl fluorescence was detected through an IR cutoff filter (Schott RG-850) by a large area (diameter 10 mm) and high gain Si-avalanche photodiode (APD; model 394-70-72-581; Advanced Photonix, Inc., USA). Decomposition of the kinetics of fluorescence relaxation and absorption changes into the sum of monoexponential functions was carried out using Marquardt's least square method.

Results

Induction followed by relaxation of BChl fluorescence

The kinetics of induction of BChl fluorescence upon rectangular shape of laser diode excitation and subsequent dark relaxation are shown in intact cells of photosynthetic bacteria *Rba. sphaeroides*and *Rsp. rubrum* under various conditions (Fig. 2). The fluorescence induction is described by a monotonous rise from the initial (dark-adapted) F_0 level to a maximum of F_{max}. Although the traces are clearly not monoexponential and show stretched kinetics, characteristic (OJIP) transients as observed routinely in fast Chl a fluorescence induction of photosystem II (Stirbet and Govindjee 2012) cannot be identified. In *Rsp. rubrum*, the rise of fluorescence yield coincides to that of light-induced P+ measured by absorption change at 796 nm (Fig. 2c). The initial magnitude of the relaxation corresponds to the fluorescence level of the induction where the excitation terminated. The longer is the excitation, the slower is the relaxation of the fluorescence (Fig. 2a). The kinetics of the relaxation follows the dark re-reduction of P+ monitored by absorption changes at 796 nm (Fig. 2c) and is exposed to similar changes as the P+ decay after treatments of the donor side of the RC (Fig. 2b), whereas external donors (reduced TMPD or ferrocene) to P+ in large excess accelerate the relaxation of the fluorescence, the cyt bc_1 inhibitors (antimycin and myxothiazol) slow down the dark decay significantly. Similar dramatic effects on the fluorescence induction cannot be seen, as only minor changes of the fluorescence maximum can be observed (Fig. 2b left panel). The fluorescence relaxation seems to be more sensitive to modification of the donor side electron transfer reactions in these native cells than the fluorescence induction.

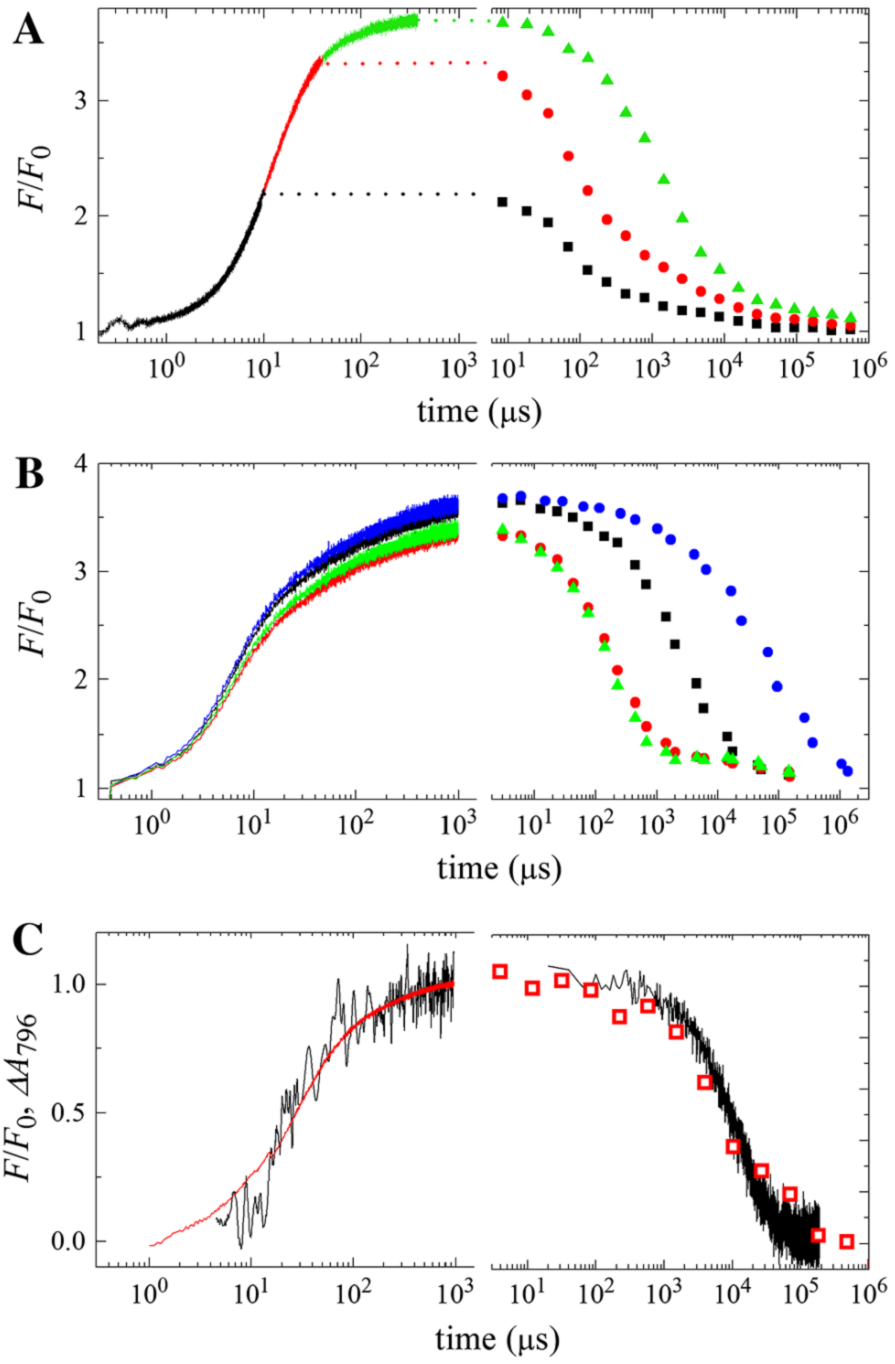

Fig. 2 Kinetics of induction and relaxation of BChl fluorescence during and after laser diode excitation, respectively, in intact cells of *Rba. sphaeroides*(a and b) and Rps. rubrum (c). Note the logarithmic time scale. The fluorescence intensity (F) is normalized to the initial (dark-adapted) value F_0. The kinetics of relaxation is sensitive to the duration of flash excitation (a), to external electron donors ferrocene (red circle, 200 μM) and reduced TMPD (green triangle, 5 mM), and to cyt bc_1 inhibitor myxothiazol (blue circle, 20 μM) (b). The kinetics of variable fluorescence induction (red line) and relaxation (red squares) coincide with the rise and decay of laser diode-induced absorption change at 796 nm (black lines) normalized to variable fluorescence (c)

Relative fluorescence yields of the closed states of the RC

As BChl fluorescence and photochemistry are complementary processes, the fluorescence relaxation reflects the conversion of closed $P^+Q_A^-$ states of the RC with maximum relative yield of 1 to open PQ_A states with relative yield of 0. The relaxation includes not only the changes of the concentrations of the open/closed RCs but the fluorescence yields of the transient (partly closed P^+Q_A and PQ_A^-) RCs, as well. Although the excitons in the

antenna cannot be trapped photochemically by any of these RCs, they can quench the BChl fluorescence. According to Kingma et al. (1983), the fluorescence yield of the PQ_A^- state is 60 % of that of the P^+Q_A in whole cells of *Rsp. rubrum*. It is argued that the losses of the excitons in the state PQ_A^- (e.g., triplet formation) are higher than those caused by fluorescence quenching by P+ in the P^+Q_A redox state of the RC. To determine the fluorescence yields attributed to the (photochemically) closed states, the cytochrome-less mutant of *Rba. sphaeroides*(CYCAI) was used. The electron transfer through the RC was controlled by external donor (reduced TMPD) and inhibitor of interquinone electron transfer (terbutryn) (Fig. 3). In lack of proper electron donor to P+, slow decay of fluorescence due to P^+Q_A state with lifetime of 700 ms can be observed in untreated RC. Addition of terbutryn to the cells increases the fluorescence yield and accelerates the relaxation of fluorescence to 70-ms lifetime that agrees with that of the $P^+Q_A^-$ → PQ_A recombination detected by absorption change measurement at 798 nm (not shown). Similarly, but with larger extent, the relaxation of fluorescence can be accelerated to 0.43-ms lifetime by addition of external electron donor (reduced TMPD) to the bacterium. Between the two kinetics, a relatively large kinetic gap exists which is suited to trap the redox state PQ_A^- of the RC by adding both terbutryn and TMPD to the culture. The kinetics drops in two steps showing that the fluorescence yield belonging to PQ_A^- redox state of the RC is about half of that of the P^+Q_A state.

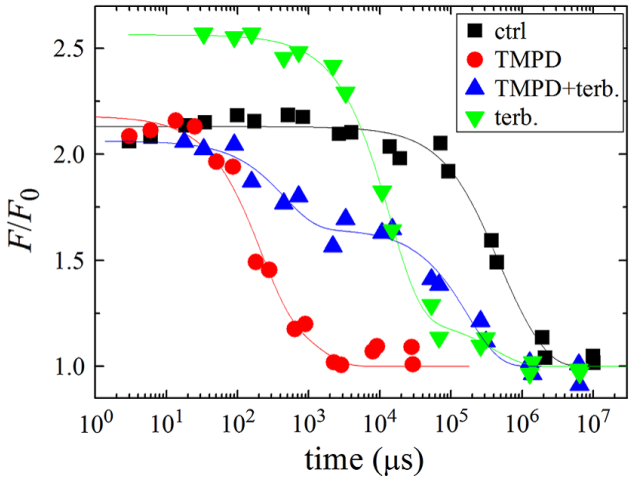

Fig. 3 Kinetics of BChl fluorescence relaxation after laser diode excitation of 40-ls duration and 808-nm wavelength in intact cells of cyt c_2 less mutant of *Rba. sphaeroides*(CYCAI). The fluorescence intensity (F) of the monitoring flashes of 3-ls duration is referred to that measured without laser diode excitation (F_0). Symbols and apparent lifetimes: untreated cells (black squares, 0.7 s), + 100 µM terbutryn (green inverted triangle, 70 ms), + 5 mM (reduced) TMPD (red circle, 430µs), and 100 µM terbutrin and 5 mM TMPD together (blue triangle, 430µs and 100 ms)

Redox titration of the flash-induced absorption change and fluorescence relaxation in Rba. sphaeroides

Flash-induced changes in intact cells of *Rba. sphaeroides*are sensitive to the actual redox potential that can be demonstrated by simultaneous equilibrium redox titrations of the relaxation of the BChl fluorescence and absorption change at 798 nm (Fig. 4). The redox changes have proved to be reversible in the 150–450 mV redox range mediated by a set of redox mediators described in ‘‘Materials and methods’’ section without significant modification of the observed kinetics. The dimer of the RC and its natural electron donor, cytochrome c_2 are the two major redox agents that might determine the redox properties of lightinduced changes of the bacterium in this redox region. Upon increase of the actual redox potential, both the amplitude and the half-time of the decay of the absorption change at 798 nm become smaller, indicating the increasing degree of oxidation of P and its donor cyt c_2^{2+} in the dark, respectively. The dark equilibrium redox titration of the amplitude can be fitted by a one-electron Nernst curve with $E_{m,P}$ = 436 mV midpoint redox potential which is significantly lower than that measured in isolated RC [495 mV at pH 8 (Maróti and Wraight 1988)]. The equilibrium redox titration of the fluorescence relaxation demonstrates the contributions of the two redox centers, as well. The measured kinetics are complex showing the presence of more components. They are shifting to longer time ranges and the amplitudes become smaller upon increase of the actual redox potential indicating the apparent decrease of the electron donation rates to light-induced P+ and oxidation of P in the dark, respectively. At the largest applied redox potential (E_h = 408 mV), all of cyt c_2 (and ~20 % of P) are oxidized in the dark and slow side reactions (e.g., charge recombination)

remain as limiting kinetic processes to eliminate the light-induced P+. Accordingly, the decomposed kinetics represents P+ reduction by reduced cyt c_2 (fast) and by side reaction (slow). The observed rate constant is $k_{obs} = k_c[\text{cyt } c_2^{2+}] + k_s$. Assuming pseudo first order kinetics between P+ and cyt c_2^{2+}, the rate constant of the fast component of the kinetics ($k_f = k_c[\text{cyt } c_2^{2+}]$) should be proportional to the actual concentration of cyt c_2^{2+} before the flash. The redox titration of k_f fits to a oneelectron Nernst curve with a redox midpoint potential of $E_{m,cyt}$ = 327 mV. The rate constant of the slow component (k_s) does not depend on E_h in the investigated range of the redox potential.

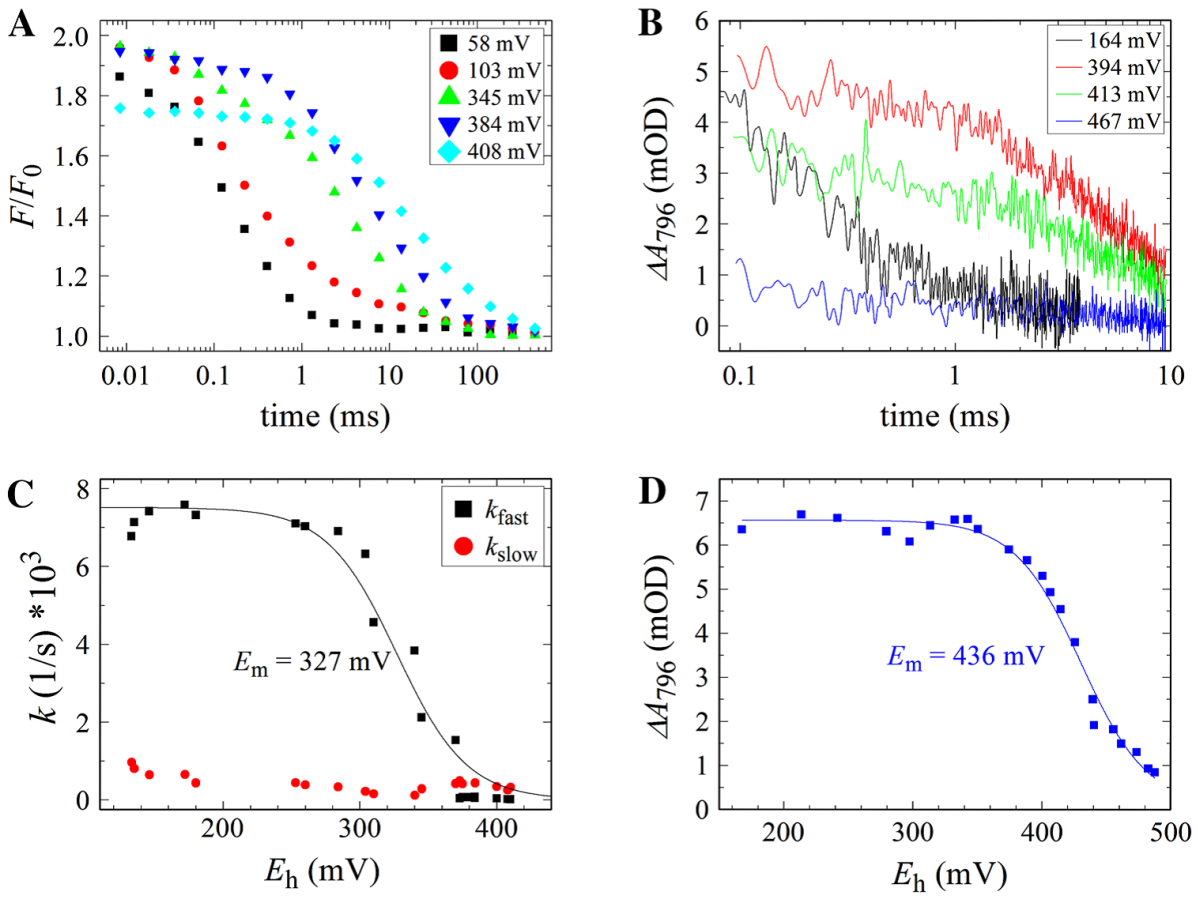

Fig. 4 Equilibrium redox titration of fluorescence induction (a) and flash-induced absorption change at 796 nm (b) of intact cells of Rba. sphaeroides. The rate constants of the fast (black squares) and slow (red circles) components of the fluorescence relaxation (c) and the amplitudes of the absorption changes (blue circles, DA_{796}, d) are plotted against the actual redox potential E_h and the redox midpoint potentials for the cyt c_2^{2+}/cyt c_2^{3+} (c) and P/P+ (d) redox couples were obtained from a fit with the one-electron Nernst function. Conditions: redox mediators: ferro- and ferricyanide (2 mM); TMPD, DAD, and DQ (20 µM); PES and PMS (1 µM) and piocyanine and etylpiocyanine (2 µM), pH 7, room temperature, and laser diode duration 200 us

Effect of the redox states of the pools on the kinetics of fluorescence relaxation

The kinetics of re-opening of the RC in the dark depends directly on the rate constants of re-reduction of P+ and reoxidation of Q_A^-. These rate constants, however, are sensitive to the rates of subsequent electron transfer steps, consequently to the redox conditions of the quinone and cyt c_2 pools. The indirect effect can be demonstrated by several ways.

Flash duration (Fig. 5)

In CYCAI mutant cell, the kinetics is not much influenced by flash duration and it remains always slow (Fig. 5a). In bacteria, where mostly the acceptor side (quinone) reactions determine the fluorescence relaxation (*Rvx. gelatinosus*), we experience about one order of magnitude slower decay if the flash duration is increased from 20µs to 1 ms (Fig. 5b). In *Rba. sphaeroides*and *Rsp. rubrum*, where the limitation of the re-opening depends mainly

on donor side reactions, the deceleration is more pronounced and the progressive appearance of a slow component in the kinetics is straightforward (Figs. 5c, d). The fluorescence relaxation curves offer hint about the extent and differences of the donor and acceptor side capacities in strains of donor and acceptor limitations, respectively.

Reduction with Na-dithionite

A convenient way of progressive reduction of the quinone pool is the addition of reducing agent Na-dithionite to the bacterium. The fluorescence relaxation becomes more complex with striking increase of the slow component(s) (not shown). In large excess of the Na-dithionite (20 mM), the initial magnitude drops and the kinetics flattens in agreement with the expectations of reduction of the pool quinones and Q_B together with partial reduction of Q_A, as well. The reduction of the acceptor side results in decrease of the photoactive RC, the variable fluorescence, and the rate of fluorescence relaxation.

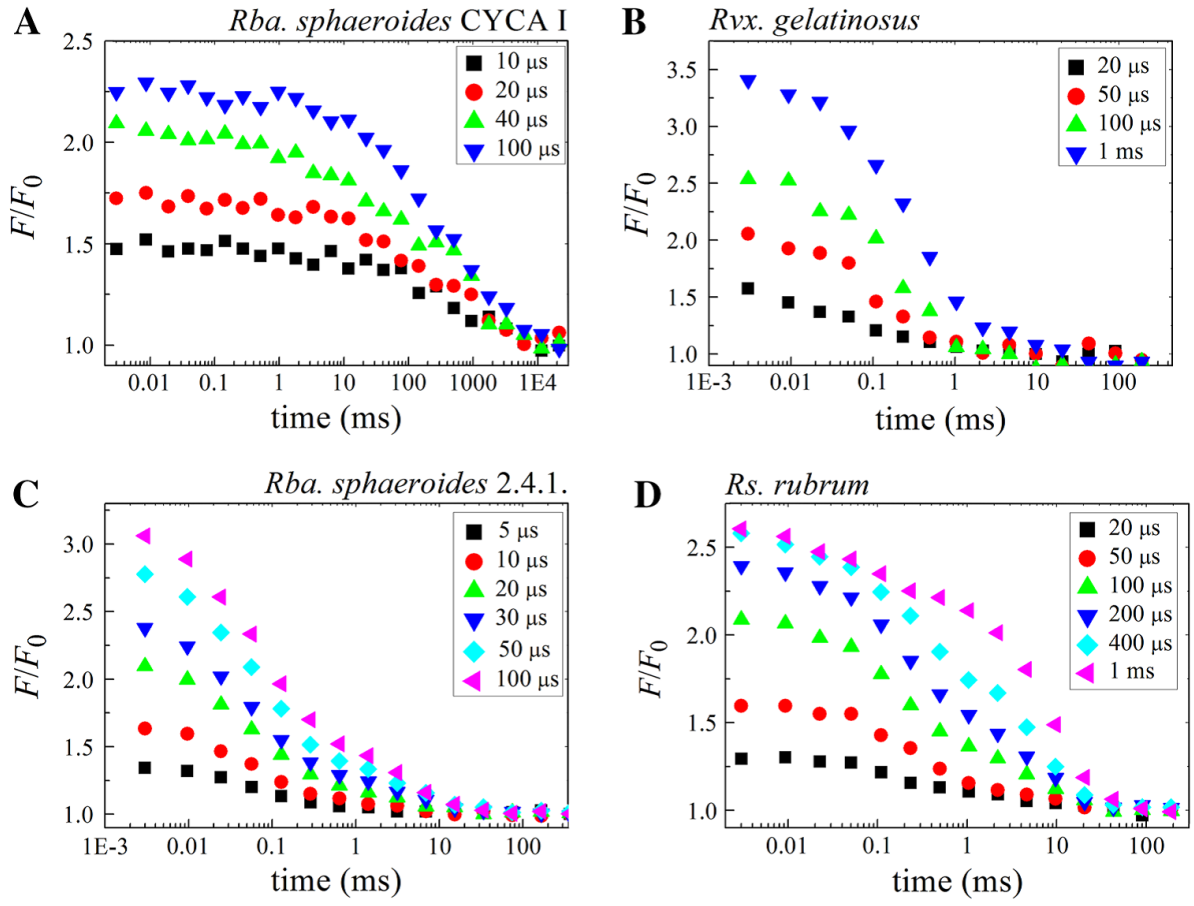

Fig. 5 Kinetics of relaxation of BChl fluorescence after laser diode excitation of variable duration (as indicated on the panels) in intact cells of cyt c_2 less mutant CYCAI of *Rba. sphaeroides*(a), *Rvx. gelatinosus* (b), *Rba. sphaeroides*wild type 2.4.1 (c), and *Rsp. rubrum* (d)

Cyt bc_1 inhibitor

The cyclic electron flow between the two redox proteins RC and cyt bc_1 assures the regeneration of the initial redox state of the pools (Fig. 1). If the function of cyt bc_1 is blocked by the inhibitors antimycin or myxothiazol, then the reduction/oxidation power of the pools would be exhausted earlier after prolonged excitation. Under these conditions, decelerated relaxation of the fluorescence is measured (Fig. 2b). Here, the fluorescence was excited for 1 ms, which is long enough for several turnovers of the RC to take place and to see the effect of blocked cyclic electron transfer on the kinetics of the fluorescence relaxation. In a control experiment without cyt bc_1 inhibitor, the decay was faster and could be accelerated further by addition of external fast electron donor (reduced TMPD) in excess to the culture. In this case, the addition of myxothiazol to the sample does not slow down the fast

relaxation of fluorescence indicating the presence of large pool of external electron donors that is independent on the function of the cyt bc_1 complex.

Effect of temperature on the kinetics of fluorescence relaxation

The decays of the relative yield of BChl variable fluorescence in *Rba. sphaeroides*and *Rvx. gelatinosus* perform characteristic changes in the physiological temperature range (Fig. 6). After 1-ms excitation of the *Rba. sphaeroides*cells, the initial relative yield is significantly larger at lower (5 C) temperature, than at higher (36 C) temperature: F_{max}/F_0 = 3.1 and 2.5, respectively. The change is about 30 %. Upon temperature increase, the kinetics remains extended (multiphasic) but shifts significantly (by more than one order of magnitude) to shorter time range: the apparent half-time is about 1 ms at 5 C and 100μs at 36 C. The changes are reversible. Similar temperature dependence can be observed in *Rvx. gelatinosus*. After decomposition of the relaxation kinetics into two exponentials, the activation enthalpies can be determined from Arrhenius representation and values of 28 and 45 kJ mol^{-1} were obtained for the fast and slow components, respectively. The slow phase is more sensitive to temperature changes than the fast phase.

Interquinone electron transfer in Rvx. gelatinosus

Due to the cytochrome subunit attached to the RC in *Rvx. gelatinosus*, the re-opening of the closed RC should be limited by the rate of the interquinone electron transfer. To determine the opening time, the cells were excited by two saturating Xe flashes with variable delay and the electrochromic absorption change at 540 nm was detected (Fig. 7a). The amplitude of the electrochromic change after the second flash progressively increased upon increase of the delay time between the two flashes and converged to that measured after the first flash (Fig. 7b). An opening time of 350μs could be deduced. We attribute this value to the electron transfer time from Q_A^- to Q_B in whole cells of *Rvx. gelatinosus*. The Q_B site inhibitors are expected to decelerate the reopening of the RC in strains of acceptor side limitation. Indeed, upon addition of terbutryn, a potent inhibitor of interquinone electron transfer in isolated RC, the complex decay of fluorescence became slower (Figs. 7c, d). The rate constant of the fast component of the relaxation was not very much affected by the inhibitor but the weight of the slow component increased dramatically (*Rvx. gelatinosus*, Fig. 7c). The same tendency but smaller changes were experienced in *Rba. sphaeroides*(Fig. 7d). Similar alterations of the kinetics were observed with other interquinone electron transfer inhibitors as o-phenantroline, stigmatellin, and atrazine (data not shown). For quantitative evaluation of the increase of the slow phase in Rba. sphaeroides, one has to take into account, that (1) disregarding the small (~20 %) fraction of RCs with ultrafast (<1μs) P+ rereduction, the rate limiting step of the fluorescence relaxation is not the interquinone electron transfer but the reduction of P+ and (2) the relative fluorescence yield corresponding to the P^+Q_A state is twice as large as that belonging to the PQ_A^- redox state of the RC (see Fig. 3). The comparison of the effect of terbutryn to the fluorescence relaxation kinetics in *Rvx. gelatinosus* and *Rba. sphaeroides*indicates that the occupation (residence) time of terbutryn at the Q_B site is limited by strict competition of quinone species of the pool in intact cells.

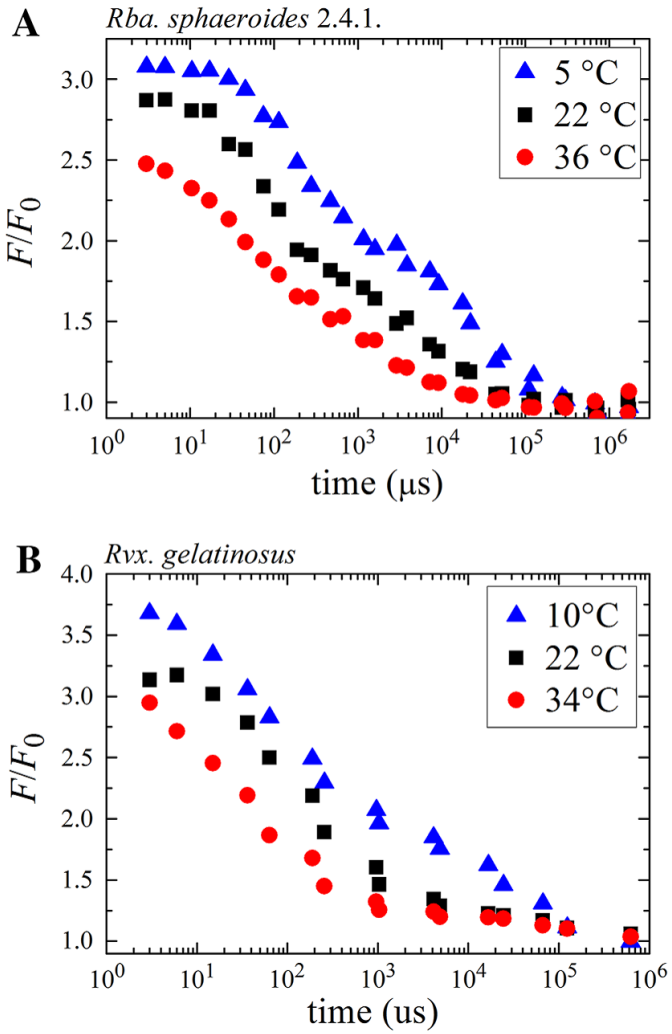

Fig. 6 Temperature dependence of the kinetics of fluorescence relaxation of whole cells of *Rba. sphaeroides*strain 2.4.1 (a) and *Rvx. gelatinosus* (b) after laser diode excitation of 50µs duration in the physiological temperature range. Note the changes both in amplitudes and decay times

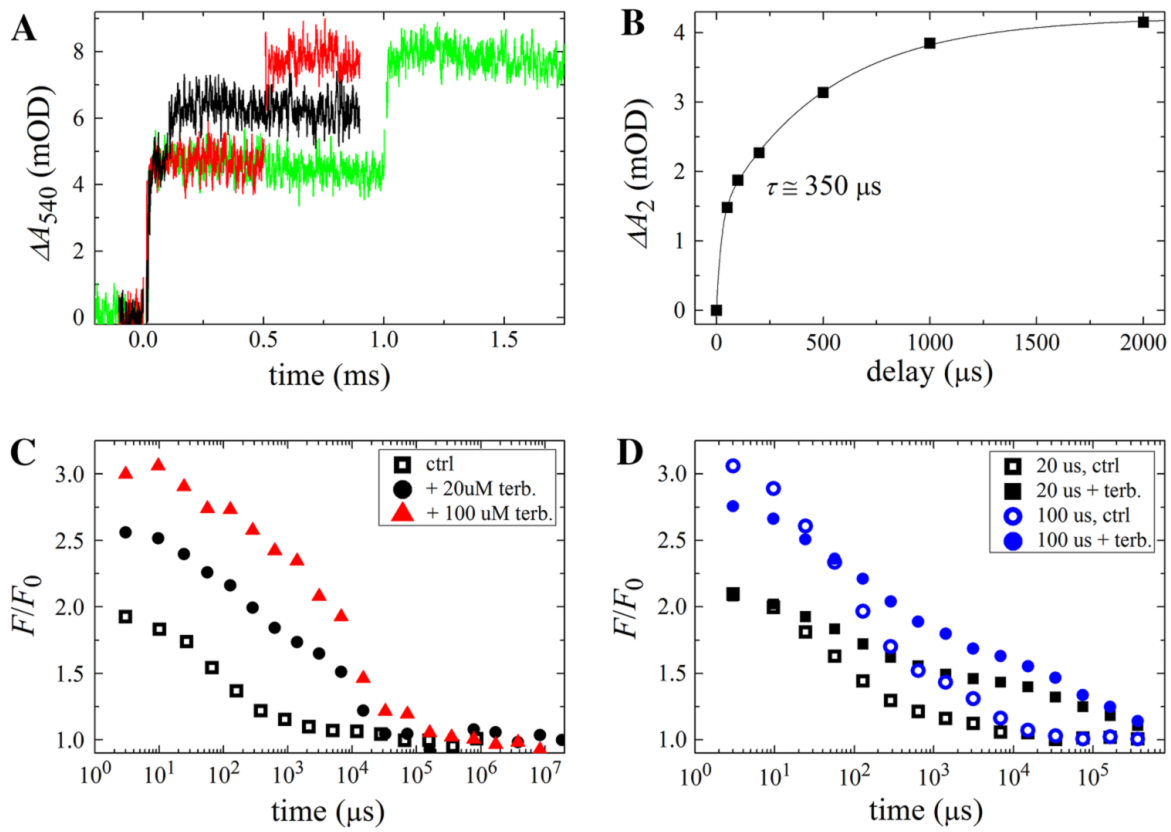

Fig. 7 Kinetics of electrochromic band shift induced by two saturating Xe flashes of duration 5µs with variable delay measured by absorption change at 540 nm in intact cells of *Rvx. gelatinosus* (a), absorption change due to the second flash (DA_2) as a function of the time gap between the first and second flashes (b) and modification of the fluorescence relaxation kinetics by Q_B site inhibitor terbutryn in *Rvx. gelatinosus* (c) and *Rba. sphaeroides*(d). The duration of laser diode excitation is 10µs (c) and the terbutryn concentration is 120 uM (d)

Discussion

The experiments above aimed to reveal phenomena determining the complex behavior of the BChl fluorescence relaxation. The yield of the fluorescence decayed monotonously in all of the investigated strains and performed no transient increase (i.e., re-closure of the RC) in the dark as reported earlier (Kolber et al. 1998; Falkowski et al. 2004; Koblizek et al. 2005). The decay kinetics gives information about the process of opening of the closed RCs that can be closed either on the donor or on the acceptor sides or on both. The opening of the donor side is controlled directly by the redox states and structural arrangement of the cytochromes [short (<1 ms) excitation] and indirectly by the rate of cyclic electron transfer [long ([1 ms) excitation]. While CYCAI (with no cyt c_2 mobile carriers) and Bla. viridis and *Rvx. gelatinosus* (with cytochrome subunit attached to the RC) are the two extreme cases, *Rba. sphaeroides*and *Rsp. rubrum* are the intermediate cases with mobile cyt c_2 species partly bound to the proximal site of the RC or not, respectively. The opening of the acceptor side depends on the redox properties and availability of the quinones at the secondary binding site (Q_B) and in the pool. It is usually much faster than the opening of the donor side unless bound cytochrome subunit (Bla. viridis and *Rvx. gelatinosus*) or proximal cyt c_2 (Rba. sphaeroides) to the RC are available. The observed difference of the relative fluorescence yields of the partly open (P^+Q_A and PQ_A^-) RC states makes the evaluation of the relaxation kinetics more complicated. The discussion will focus to the kinetics and energetics of donor and acceptor side electron transfer reactions that determine the fluorescence relaxation in intact cells of *Rba. sphaeroides*and *Rsp. rubrum* and *Rvx. gelatinosus*, respectively.

P^+ re-reduction plays major role in fluorescence relaxation of Rba. sphaeroidesand Rsp. rubrum

In native RC, fast electron transfers occur on both the donor and acceptor sides in order to prevent the dissipation of the absorbed light energy by recombination of the lightinduced charges in the RC. If the pathways of the electron

transfer are blocked [e.g., by cyt c_2-less mutation (CYCAI) or by reduction of the quinone pool by dithionate], the increase of the delayed fluorescence is a good indication of wasteful charge recombination (Asztalos and Maróti 2009). In native cells of Rba. sphaeroides, the kinetics of reopening of the closed RC are determined by the rates of P+ reduction and interquinone electron transfer. In isolated RC of Rba. sphaeroides, the first interquinone electron transfer is conformational gated and is significantly faster (1–100μs) than the proton-activated second electron transfer [~1 ms at pH 8 (Wraight 2004; Wraight and Gunner 2009)]. In chromatophore membrane of Rba. capsulatus, Lavergne et al. (1999) found that the first and second interquinone electron transfers exhibited essentially identical kinetic properties both with rates in the $100\mu s^{-1}$ range including the associated protonation reactions. These include by far the fastest step in quinone turnover of the acceptor side of the RC that takes about 1.6 ms (Comayras et al. 2005). In re-reduction of P+ following a saturating flash in intact cells of Rba. sphaeroides, at least three phases were observed in agreement with earlier studies on purified partners (Drepper et al. 1997; Tetreault et al. 2001), on isolated chromatophores (Overfield et al. 1979) and intact cells (Bina et al. 2009). The multiphasicity of the P+ reduction kinetics can be interpreted either by the proximal–distal binding model (Moser and Dutton 1988; Gerencse ´r et al. 1999; Larson and Wraight 2000) or by the confinement of a single cytochrome c_2 in a supercomplex of two RCs and one cytochrome bc_1 complex (Joliot et al. 1989; Lavergne et al. 2009). The ultrafast (~1μs) phase could not be resolved here but we managed to estimate its contribution by double flash excitation: the amplitude amounted about 20–30 % of the total. This component corresponds to RCs where the cyt c_2 is bound at a proximal site. The second phase, in the 20–200μs range, had larger amplitude. Its origin has been debated: possibly a binding of the cyt c_2 on a distal site of the RC, or encounter complex, or jump from other binding sites (e.g., cyt bc_1). It seems some of its features appear first-order (concentration-independent rate) and some simply diffusion (rate dependence on viscosity). The third phase (100μs–10 ms) involves reactions with not bound cyt c_2 and/or reactions with the cyt bc_1 complex (shuttling of the cyt c_2 between both complexes), because of the RC:cyt c_2 stoichiometric excess. Using a subsaturating flash would accordingly suppress this component (Asztalos et al. 2012). The kinetics of the slow phase reflects the key redox reactions taking place in the cyt bc_1 complex. The flash induced bifurcated oxidation of ubiquinol in the cyt bc_1 complex leads to the reduction of heme b_h at 1.5–2 ms and the rereduction of cyt c_1 by ubiquinol, the generation of membrane potential, and the proton release into the chromatophore interior take about 10–20 ms (Mulkidjanian 2005). The slow phase of P+ reduction is severely blocked by cyt bc_1 inhibitors. We found close correlation between the equilibrium redox titration of the donor side of the RC and the fluorescence relaxation that supported the determining role of P+ reduction as the rate-limiting step of re-opening of the RC in Rba. sphaeroides. The measured midpoint redox potential of 327 mV for the cyt c_2^{3+}/cyt c_2^{2+} redox couple in the native cell showed fair agreement with earlier data obtained under different conditions. A midpoint redox potential of 345 mV was obtained in chromatophores of *Rba. sphaeroides*(Meinhardt and Crofts 1982) and in solution (Pettigrew et al. 1975; Prince and Bashford 1979). The same value was used in the studies by Lin et al. (1994) and Venturoli et al. (1998). A slightly different value of 335 mV was offered for free cyt c_2 from *Rba. sphaeroides*in solution at pH 8.0 (Drepper et al. 1997). Cross-linking of cyt c_2 to the RC affected the redox properties of the heme, leading to an E_m value of 370 mV between pH 7.5 and 9.5 (Drepper et al. 1997). By changing the duration of excitation, the number of turnovers and therefore the degree of light saturation could be systematically modified. At high laser diode intensity, the half-time of the fluorescence induction was as low as about 10μs, about two orders of magnitude smaller than the transit time of cyt c_2 between the cyt bc_1 complex and the RC. The analysis of the variation of the fast and slow components of the yield of the variable fluorescence upon flash duration offered a relatively small cyt c_2 pool (or cyt c_2:RC stoichiometric ratio) of the membrane. This is in agreement with results of other functional and structural studies offering few mobile cyt c_2 carriers and cyt bc_1 complexes [[cyt c_2]/[RC] ~ 0.5 and [cyt bc_1]/[RC] ~ 0.5] in *Rba. sphaeroides*grown under anaerobic photosynthetic conditions (Cartron et al. 2014). The cytochromes are much less than ubiquinones that are in large excess [typically [UQ]/[RC] ~ 20–30]; therefore, the redox capacity of the donor side is much more limited than that of the acceptor side of the RC. The exact stoichiometric ratios depend on the strains and growing conditions (light intensity, oxygen tension, etc.). In contrast to Rba. sphaeroides, *Rsp. rubrum* has no tightly bound cyt c_2 to the RC. The positively charged Arg32 residue of cyt c_2 is present in the *Rba. sphaeroides*but not in *Rsp. rubrum*. Thus, the electrostatic interaction with negatively charged residues on the RC is removed and the affinity of cyt c_2 to RC becomes less in *Rsp. rubrum* (Paddock et al. 2005). Accordingly, the reduction of P+ occurs significantly slower in *Rsp. rubrum* than in *Rba. sphaeroides*and much slower than the interquinone electron transfer. In accordance with the slower opening of the RC on the donor side, the fluorescence yield starts to relax after correspondingly longer lag phase. In this species, the fluorescence yield is governed entirely by P+. Indeed, the correlation between the yield of variable fluorescence and concentration of oxidized donor could be nicely demonstrated by simultaneous measurements of absorption change at 798 nm and induction and relaxation of fluorescence during and after rectangular shape of laser diode excitation, respectively. The close

correlation is preserved on wide time scale using excitations flashes attenuated by gray filters. Similar results can be obtained with cytochrome-less mutant of Rba. sphaeroides. The gap between the absorption and fluorescence kinetics can be used to quatify the connectivity of the photosynthetic units in the bacterial membrane (Lavergne and Trissl 1995; Rivoyre et al. 2010; Maróti et al. 2013). Direct and indirect evidences show that the kinetics of fluorescence relaxation reflects the re-reduction of P+ in these strains and the acceptor side should have a minor role. This is in strong contradiction with interpretation of chlorophyll fluorescence dark relaxation observed in higher plants where the re-reduction of the oxidized chlorophyll dimer (P680+) by the secondary donor (tyrosine 161 of the D_1 subunit of PSII) is much faster ($[1\mu s)^{-1}$ than any of the electron transfer reactions in the acceptor side. The rereduction of P680+ can be made responsible for re-opening the RC (Cser and Vass 2007). Earlier fluorescence relaxation studies on bacterial systems were interpreted similarly. It was argued that the complex kinetics of relaxation could be entirely described by the electron export from the acceptor side of the RC (Kolber et al. 1998). This view was utilized to understand the organization of the photosynthetic apparatus during transition form aerobic to anaerobic conditions (Koblizek et al. 2005) but not in Kis et al. (2014).

Acceptor side limitation of fluorescence relaxation in Rvx. gelatinosus

As the cytochrome subunit assures very fast reduction of P+ after one or two photon hits of the RC, the electron transfer in the acceptor side will limit the re-opening of the RC during short excitation. Using double flash experiment, we estimated the $Q_A^- \rightarrow Q_B$ electron transfer rate as $350\mu s^{-1}$. For longer excitation when the RC performs multiple turnovers, the rates of the donor side reactions will be smaller, become comparable to that of the acceptor side reactions and contribute to the rate limitation. The acceptor side limitation is supported by the sensitivity of the rate of fluorescence relaxation to acceptor side inhibitors. Terbutryn, a well-known interquinone electron transfer inhibitor had more dramatic decelerating effect on the relaxation in *Rvx. gelatinosus* than in Rba. sphaeroides. Additionally, the inhibitors modify the initial and maximum yields of the fluorescence induction: F_0 is increased and F_{max} is decreased making the variable fluorescence smaller. Whether the inhibitors disconnect the photosynthetic units, or favor the accumulation of Q_A^- in the dark (both effects lead to increase of F_0) and/or do not allow the reduction of the ubiquinone pool by light excitation (decrease F_{max}), are not yet answered questions. In isolated RCs, the inhibitors (terbutryne, stigmatellin, atrazine, and o-phenantroline) block the interquinone electron transfer by competing with the ubiquinones for the Q_B binding site. Our fluorescence assays demonstrated that the inhibitory effect of these chemicals in whole cells was not very effective as the block of the acceptor side was kinetically limited. They inhibit the growth of the bacteria in culture under stationary illumination of low or moderate intensity. A reasonable explanation of the observation is that under our conditions (nitrogen atmosphere and long dark adaptation), the cells are under partly reducing state and the majority of the Q_B in the RC is in semireduced form, Q_B^-. Because it has large binding affinity to the RC [in isolated RC, UQ_{10}^- has about 10 times larger binding constant to the RC than UQ (Wraight 2004)], the direct binding of the inhibitor in the dark is prohibited. The inhibitor has chance to compete for the secondary quinone binding site when the semiquinone is double reduced and leaves the RC. However, after prolonged illumination, the quinone pool becomes more reduced and the competition of the inhibitor with QH_2 becomes unfavorable. Additionally, the quinol at the Q_B site can disproportionate ($Q_AQH_2 \leftarrow\rightarrow Q_A^-Q_BH + H^+$) resulting in semiquinone of high binding affinity to the Q_B binding site (Maróti and Wraight 2008).

Activation barriers of the rate-limiting steps of the fluorescence relaxation

Both the yield and the rates of relaxation of BChl fluorescence showed temperature dependence in our experiments. The observed alteration of the fluorescence yield can be explained by assuming variable exposure of the BChl molecules located in the lipid membrane (high yield of fluorescence) to the aqueous environment (low yield of fluorescence) upon temperature change. The concept was introduced and worked well in algae and higher plants (Murata and Fork 1975). The interpretation of the large temperature dependence of the apparent rate of relaxation, however, seems to be more difficult. It should not involve a simple diffusion-controlled process but a limiting reaction with considerable activation barriers of 28 and 45 kJ mol^{-1} for the fast (~200μs) and slow (~2 ms) components, respectively. As the reactions of the quinone reduction and cytochrome oxidation on the acceptor and donor sides of the RC, respectively, exhibit distinct activation enthalpies, the temperature dependence may serve as selection among dominating reactions in the kinetics. The electron transfer reactions in the acceptor quinone complex of the isolated RC are slowing down while the temperature is lowered, i.e., they exhibit significant activation enthalpy. High activation enthalpies (~60 kJ mol^{-1}) were reported both for the first electron transfer ($Q_A^-Q_B \rightarrow Q_AQ_B^-$, Mancino et al. 1984; Gopta et al. 1997) and for the second proton uptake ($Q_AQ_BH^- \rightarrow Q_AQ_BH_2$, Gopta et al. 1998). The interquinone electron transfer has been described as gated reaction where not the electron

transfer itself but changes in quinone position (distal and proximal to Fe^{2+}) or protein conformation (including protonation) are the rate limiting step (Graige et al. 1998; Mulkidjanian 2005; Wraight and Gunner 2009). The high activation barriers of ubiquinone reduction seem to be coupled to these reactions that prevent the potentially detrimental reversion of the interquinone electron transfer. Similarly to the quinone reduction in the RC, the bifurcated oxidation of ubiquinol in the cyt bc_1 complex has high activation energy (Hong et al. 1999). In contrast to the acceptor side, the donor side reactions associated with P+ re-reduction by cyt c_2 $^{2+}$ (either in proximal or distal binding sites) have significantly smaller activation enthalpies. Values of 11.7 and 8.0 kJ mol^{-1} were obtained for the very fast (half-life< 1μs) and fast (half-life 60μs) P+ reduction by covalently bound cyt c_2 in isolated RC of Rba. sphaeroides, respectively (Drepper et al. 1997). Even smaller activation energies were reported for Bla. viridis where a tetraheme cyt c complex as subunit was bound to the RC: values of 6.9, 3.8, and 4.3 kJ mol^{-1} were measured when one, two, and three hemes were reduced, respectively (Mathis et al. 1994). In intact cells of Rba. sphaeroides, the major fraction of P+ reduction is due to loosely bound cyt c_2 with half-life of ~100μs (fast) and 2–10 ms (slow) and small activation energies. We observed that the activation energy of the dominating fast fluorescence relaxation with 100–200μs half-time was moderately small (28 kJ mol^{-1}). The slow component with 2–5 ms half-time, however, had higher activation barrier (45 kJ mol^{-1}) indicating the contributions of the acceptor side and cyt bc_1 complex that are characterized by higher activation enthalpies. It is supported by the observation that the slow component exhibits larger sensitivity to terbutryn, flash duration, and cyt bc_1 inhibitor than the fast phase of the relaxation. The investigations on activation barriers confirm the essential message of this study: the donor side electron transfer reactions dominate the kinetics of the fluorescence relaxation in *Rba. sphaeroides*after short (<100μs) excitation (close to single turnover) and the contribution of the acceptor side enhances after long excitation (multiple turnovers).

Acknowledgments

Thanks to TA ´ MOP 4.2.2.A-11/1KONV-2012- 0060, TA ´ MOP 4.2.2.B, and COST Actions on ‘‘Understanding Movement and Mechanism in Molecular Machines’’ (CM1306) programs for financial support.

References

Asztalos E, Maróti P (2009) Export or recombination of charges in reaction centers in intact cells of photosynthetic bacteria Biochim Biophys Acta 1787:1444–1450

Asztalos E, Kis M, Maróti P (2010a) Aging photosynthetic bacteria monitored by absorption and fluorescence changes. Acta Biologica Szegediensis 54:149–154

Asztalos E, Italiano F, Milano F, Maróti P, Trotta M (2010b) Early detection of mercury contamination by fluorescence induction of photosynthetic bacteria. Photochem Photobiol Sci 9:1218–1223

Asztalos E, Sipka G, Kis M, Trotta M, Maróti P (2012) The reaction center is the sensitive target of the mercury(II) ion in intact cells of photosynthetic bacteria. Photosynth Res 112:129–140

Bahatyrova S, Frese RN, Siebert CA, Olsen JD, van der Werf KO, van Grondelle R, Niederman RA, Bullough PA, Otto C, Hunter CN (2004) The native architecture of a photosynthetic membrane. Nature 430:1058–1062

Bina D, Litvin R, Va ´cha F (2009) Kinetics of in vivo bacteriochlorophyll fluorescence yield and the state of photosynthetic apparatus of purple bacteria. Photosynth Res 99:115–125

Blankenship RE, Madigan MT, Bauer CE (eds) (1995) Anoxygenic photosynthetic bacteria. Kluwer Academic, Dordrecht, The Netherlands Bukhov N, Egorova E, Krendeleva T, Rubin A, Wiese Ch, Heber U (2001) Relaxation of variable chlorophyll fluorescence after illumination of dark-adapted barley leaves as influenced by the redox states of electron carriers. Photosyth Res 70:155–166

Cartron ML, Olsen JD, Sener M, Jackson PJ, Brindley AA, Qian P, Dickman MJ, Leggett GJ, Schulten K, Hunter CN (2014) Integration of energy and electron transfer processes in the photosynthetic membrane of Rhodobacter sphaeroides. Biochim Biophys Acta 1837(10):1769–1780

Clayton RK (1966) Relations between photochemistry and fluorescence in cells and extracts of photosynthetic bacteria. Photochem Photobiol 5:807–821

Comayras F, Jungas C, Lavergne J (2005) Functional consequences of the organization of the photosynthetic apparatus in Rhodobacter sphaeroides: I. Quinone domains and excitation energy transfer in chromatophores and reaction center antenna complexes. J Biol Chem 280:11203–11213

Crofts A, Guergova-Kuras M, Hong S (1998) Chromatophore heterogeneity explains phenomena seen in Rhodobacter sphaeroides previously attributed to supercomplexes. Photosynth Res 55:357–362

Cser K, Vass I (2007) Radiative and non-radiative charge recombination pathways in photosystem II studied by thermoluminescence and chlorophyll fluorescence in the cyanobacterium Synechocystis 6803. Biochim Biophys Acta 1767:233–243

D’Haene SE, Crouch LI, Jones MR, Frese RN (2014) Organization in photosynthetic membranes of purple bacteria in vivo: The role of carotenoids. Biochim Biophys Acta 1837:1665–1673

Drepper F, Dorlet P, Mathis P (1997) Cross-linked electron transfer complex between cytochrome c_2 and the photosynthetic reaction center of Rhodobacter sphaeroides. Biochemistry 36:1418–1427

Falkowski PG, Koblizek M, Gorbunov M, Kolber Z (2004) Development and application of variable chlorophyll fluorescence technique in marine ecosystems. In: Papageorgiou GC, Govindjee (eds) Chlorophyll a fluorescence: signature of photosynthesis, advances in photosynthesis and respiration, 19th ednSpringer, Dordrecht, pp 757–778

Francia F, Wang JM, Venturoli G, Melandri BA, Rigaud JL, Barz WP, Oesterhelt D (1999) The reaction center-LH1 antenna complex of Rhodobacter sphaeroides contains one PufX molecule which is involved in dimerization of this complex Biochemistry 38:6834–6845

Gerencse ´r L, Laczko ´ G, Maróti P (1999) Unbinding of oxidized cytochrome c from photosynthetic reaction center of Rhodobacter sphaeroides is the bottleneck of fast turnover. Biochemistry 38:16866–16875

Gopta OA, Bloch DA, Cherepanov DA, Mulkidjanian AY (1997) Temperature dependence of the electrogenic reaction in the Q_B site of the Rhodobacter sphaeroides photosynthetic reaction center: the $Q_A^- Q_B$? $Q_A Q_B^-$ transition. FEBS Lett 412:490–494

Gopta OA, Cherepanov DA, Semenov AY, Mulkidjanian AY, Bloch DA (1998) Effect of temperature and surface potential on the electrogenic proton uptake in the Q_B site of the Rhodobacter sphaeroides reaction center: $Q_A^- Q_B^-$? $Q_A Q_B H_2$ transition. Photosynth Res 55:309–316

Graige MS, Feher G, Okamura MY (1998) Conformational gating of the electron transfer reaction $Q_A^- Q_B$? $Q_A Q_B^-$ in bacterial reaction centers of Rhodobacter sphaeroides determined by a driving force assay. Proc Natl Acad Sci USA 95:11679–11684

Photosynth Res123 Hohmann-Mariott MF, Blankenship RE (2007) Variable fluorescence in green sulfur bacteria. Biochim Biophys Acta 1767:106–113

Hong SJ, Ugulava N, Guergova-Kuras M, Crofts AR (1999) The energy landscape for ubihydroquinone oxidation at the Q_O site of the bc_1 complex in Rhodobacter sphaeroides. J Biol Chem 274:33931–33944

Joliot P, Vermeglio A, Joliot A (1989) Evidence for supercomplex between reaction centers, cytochrome c_2 and cytochrome bc_1 complex in Rhodobacter sphaeroides whole cells. Biochim Biophys Acta 975:336–345

Kingma H, Duysens LNM, van Grondelle R (1983) Magnetic fieldstimulated luminescence and a matrix model for energy transfer; a new method for determining the redox state of the first quinone acceptor in the reaction center of whole cells of Rhodospirillum rubrum. Biochim Biophys Acta 725:434–443

Kis M, Asztalos E, Sipka G, Maróti P (2014) Assembly of photosynthetic apparatus in Rhodobacter sphaeroides as revealed by functional assessments at different growth phases and in synchronized and greening cells. Photosynth Res 122:261–273

Koblizek M, Shih JD, Breitbart SI, Ratcliffe EC, Kolber ZS, Hunter CN, Niederman RA (2005) Sequential assembly of photosynthetic units in Rhodobacter sphaeroides as revealed by fast repetition rate analysis of variable bacteriochlorophyll a fluorescence. Biochim Biophys Acta 1706:220–231

Kocsis P, Asztalos E, Gingl Z, Maróti P (2010) Kinetic bacteriochlorophyll fluorometer. Photosynth Res 105:73–82

Kolber ZS, Prasil O, Falkowski PG (1998) Measurements of variable chlorophyll fluorescence using fast repetition rate techniques: defining methodology and experimental protocols. Biochim Biophys Acta 1367:88–106

Konorty M, Brumfeld V, Vermeglio A, Kahana N, Medalia O, Minsky A (2009) Photosynthetic system in Blastochloris viridis revisited. Biochemistry 48:4753–4761

Larson JW, Wraight CA (2000) Preferential binding of equine ferricytochrome c to the bacterial photosynthetic reaction center from Rhodobacter sphaeroides. Biochemistry 39:14822–14830

Lavergne J, Trissl H-W (1995) Theory of fluorescence induction in photosystem II: derivation of analytical expressions in a model including exciton-radical-pair equilibrium and restricted energy transfer between photosynthetic units. Biophys J 68:2474–2492

Lavergne J, Matthews C, Ginet N (1999) Electron and proton transfer on the acceptor side of the reaction center in chromatophores of Rhodobacter capsulatus: evidence for direct protonation of the semiquinone state of Q_B. Biochemistry 38:4542–4552

Lavergne J, Vermeglio A, Joliot P (2009) Functional coupling between reaction centers and cytochrome bc_1 complexes. In: Hunter CN, Daldal F, Thurnauer M, Beatty JT (eds) Advances in photosynthesis and respiration: the purple phototrophic bacteria Springer, Dordrecht, pp 509–536

Lin X, Williams JC, Allen JP, Mathis P (1994) Relationship between rate and free energy difference for electron transfer from cytochrome c_2 to the reaction center in Rhodobacter sphaeroides. Biochemistry 33:13517–13523

Mancino LJ, Dean DP, Blankenship RE (1984) Kinetics and thermodynamics of the $P870^? Q_A^-$? $P870^? Q_B^-$ reaction in isolated reaction centers from the photosynthetic bacterium Rhodopseudomonas sphaeroides. Biochim Biophys Acta 764:46–54 Maróti P (2008) Kinetics and yields of bacteriochlorophyll fluorescence: redox and conformation changes in reaction center of Rhodobacter sphaeroides. Eur Biophys J 37:1175–1184

Maróti P, Wraight CA (1988) Flash-induced $H^?$ binding by bacterial photosynthetic reaction centers: comparison of spectrophotometric and conductimetric methods. Biochim Biophys Acta 934:314–328

Maróti P, Wraight CA (2008) The redox midpoint potential of the primary quinone of reaction centers in chromatophores of Rhodobacter sphaeroides is pH independent. Eur Biophys J 37:1207–1217

Maróti P, Asztalos E, Sipka G (2013) Fluorescence assay for photosynthetic capacity of bacteria. Biophys J 104(2):545a

Mathis P, Ortega JM, Venturoli G (1994) Interaction between cytochrome c and the photosynthetic reaction center of purple bacteria: behaviour at low temperature. Biochimie 76:569–579

Meinhardt SW, Crofts AR (1982) Kinetic and thermodynamic resolution of cytochrome c_1 and cytochrome c_2 from Rhodopseudomonas sphaeroides. FEBS Lett 149:223–227

Moser CC, Dutton PL (1988) Cytochrome c and c_2 binding dynamics and electron transfer with photosynthetic reaction center protein and other integral membrane redox proteins. Biochemistry 27(7):2450–2461

Mulkidjanian AY (2005) Ubiquinol oxidation in the cytochrome bc_1 complex: reaction mechanism and prevention of short-circuiting Biochim Biophys Acta 1709:5–34

Murata N, Fork DC (1975) Temperature dependence of chlorophyll a fluorescence in relation to the physical phase of membrane lipids in algae and higher plants. Plant Physiol 56:791–796

Niederman RA (2006) Structure, function and formation of bacterial intracytoplasmic membranes. In: Shively JM (ed) Complex intracellular structures in prokaryotes, microbiology monographs, vol 2. Springer, Berlin, pp 193–227

Okamura MY, Paddock ML, Graige MS, Feher G (2000) Proton and electron transfer in bacterial reaction centers. Biochim Biophys Acta 1458:148–163

Overfield RE, Wraight CA, deVault D (1979) Microsecond photooxidation kinetics of cytochrome c_2 from Rhodopseudomonas sphaeroides: in vivo and solution studies. FEBS Lett 105:137–142

Paddock ML, Weber KH, Chang C, Okamura MY (2005) Interactions between cytochrome c_2 and the photosynthetic reaction center from Rhodobacter sphaeroides: the cation-p interaction. Biochemistry 44:9619–9625

Pettigrew GW, Meyer TE, Bartsch RG, Kamen MD (1975) pH dependence of the oxidation-reduction potential of cytochrome c_2. Biochim Biophys Acta 430:197–208

Prince RC, Bashford CL (1979) Equilibrium and kinetic measurements of the redox potentials of cytochromes c_2 in vitro and in vivo. Biochim Biophys Acta 547:447–454

Rivoyre M, Ginet N, Bouyer P, Lavergne J (2010) Excitation transfer connectivity in different purple bacteria: a theoretical and experimental study. Biochim Biophys Acta 1797:1780–1794

Scheuring S (2009) The supramolecular assembly of the photosynthetic apparatus of purple bacteria investigated by high-resolution atomic force microscopy. In: Hunter CN, Daldal F, Thurnauer M, Beatty JT (eds) Advances in photosynthesis and respiration: the purple phototrophic bacteria. Springer, Dordrecht, pp 941–952

Sener MK, Schulten K (2009) From atomic-level structure to supramolecular organization in the photosynthetic unit of purple bacteria. In: Hunter CN, Daldal F, Thurnauer M, Beatty JT (eds) Advances in photosynthesis and respiration: the purple phototrophic bacteria. Springer, Dordrecht, pp 275–294

Sener MK, Olsen JD, Hunter CN, Schulten K (2007) Atomic-level structural and functional model of a bacterial photosynthetic membrane vesicle. Proc Natl Acad Sci USA 104:15723–15728

Siström WR (1962) The kinetics of the synthesis of photopigments in Rhodopseudomonas sphaeroides. J Gen Microbiol 28:607–616

Stirbet A, Govindjee (2012) Chlorophyll a fluorescence induction: a personal perspective of the thermal phase, the J-I-P rise Photosynth Res 113:15–61

Sturgis JN, Niederman RA (2009) Organization and assembly of light-harvesting complexes in the purple bacterial membrane. In: Hunter CN, Daldal F, Thurnauer M, Beatty JT (eds) Advances in photosynthesis and respiration: the purple phototrophic bacteria Springer, Dordrecht, pp 253–273.